Journal of Combinatorial Mathematics
and Combinatorial Computing
www.combinatorialpress.com/jcmcc

Combinatorial Press

# Hydrochemical processes and evolutionary mechanisms of groundwater and surface water in the Anlecun mining area: a computational study based on multivariate statistical analysis and isotope techniques

Huiqian Zhang[1], Dongchuan Xue[1,✉], Jiahui Zhang1, Li Wang[1]

[1] *Faculty of Land Resources Engineering, Kunming University of Science and Technology, Kunming, Yunnan, 650093, China*

ABSTRACT

Karst water plays a vital role on population's daily needs, determining groundwater sources, chemical changes, and accurately evaluating flow paths and evolution stages is essential for proper protection and use of mining area groundwater resources. This study carried 10 sets karst groundwater and surface water samples from the Anle Village mining area. Based on multivariate statistical analysis, Piper trilinear diagrams, Gibbs diagrams, and isotopic techniques, the hydrogeochemical characteristics of karst groundwater (including contaminated and uncontaminated water samples) and surface water in the mining area were analyzed, systematically revealing their recharge sources, recharge ages, and hydrochemical evolution patterns. The results show that the uncontaminated groundwater and surface water are slightly alkaline with a prevalence of $N^{a+}$ and $Mg^{2+}$ cations with $HCO_3^-$ and $SO_4^{2-}$ anions and $HCO_3^-$-$SO_4^{2-}$-$Ca^{2+}$-$Mg^2$ and $HCO_3^-$-$Ca^{2+}$-$Mg^2$, respectively. The uncontaminated samples show the high content of impurities with dominance of $Ca^{2+}$ and $Mg^{2+}$ cations and $SO_4^{2-}$ anions. the uncontaminated karst groundwater and surface water are predominantly recharged by atmospheric precipitation and are influenced by evaporation. the uncontaminated karst groundwater and surface water is primarily driven by the weathering and dissolution of carbonate, sulfate, and silicate rocks. The $NO_3^-$ concentration in the surface water may be associated with agricultural fertilizers, and the contaminated groundwater is closely related to mineral resource development. The research results are of great significance for understanding the circulation and evolution processes of karst groundwater and surface water in the Anle Village mining area and for the protection and utilization of water resources.

*Keywords:* Karst water, Anle Village mining area, multivariate statistical analysis, Gibbs diagrams, isotopic techniques

✉ Corresponding author.
*E-mail address:* hannibalnn@163.com (D. Xue).
Received 05 March 2024; Revised 10 May 2024; Accepted 05 December 2024; Published Online 15 April 2025.
DOI: 10.61091/jcmcc127a-368

## 1. Introduction

Water resource is one of the most valuable natural resources on the earth, which is the key to maintain the natural environment and species diversity, and concerns human life and health, production and life, agricultural irrigation, industrial production and other aspects of the development of human life and health, and the possession of clean water is a necessary condition for the social and economic development of human beings [1-2], China's annual average total water resources has reached 2.76 trillion m3, ranking sixth in the world, and the per capita possession is relatively small. However, the per capita possession is relatively small, accounting for only a quarter of the world average [3-4].

In the hydrosphere equilibrium system, water bodies are transferred and circulated by evaporation, precipitation, surface runoff and subsurface runoff at different locations and on different time scales [5]. Among them, surface water and groundwater are closely connected and interact with each other, and their mutual recharge and discharge constitute the most important components of the ecosystem water cycle [6-8]. In order to understand the interaction relationship between water bodies and the environment, water bodies and water bodies, it is essential to explore the structural composition of water bodies, the formation of hydrochemical components, the characteristics of spatial distribution and their evolutionary mechanisms [9-10]. The analysis of hydrochemical characteristics and the description of physical properties and chemical characteristics of water bodies can provide theoretical support for the protection of water resources and the construction of ecological civilization [11]. In addition, the study of the causal mechanisms of hydrochemical characterization contributes to environmental monitoring, especially in assessing the impacts of industrial activities, agricultural activities and urban development on the water environment, and it can help to determine the distribution, reserves and exploitation potential of mineral and water resources [12-13]. In order to ensure the safety of water quality and human life and health, it is important to investigate the hydrochemical characteristics of groundwater and surface water and their evolutionary mechanisms, which can help to develop, utilize and protect water resources in a scientific and rational way [14].

On the other hand, water resources are often one of the main factors constraining the socioeconomic development of arid or semi-arid regions [15]. Surface water and groundwater are the most important parts of the water cycle process, and they are closely linked and independent of each other. The characteristics of chemical components of water record, to a certain extent, the source, migration and transformation of solutes in water bodies, as well as important information related to the water cycle [16-17]. It is of great practical significance to understand the hydrochemical characteristics of surface water and groundwater and their causes for the rational development, utilization and management of regional water resources [18]. The study of the hydrochemistry of surface water and groundwater in the coal mine area can also help to analyze and prevent water hazards in the mines, which can provide reference for the safe mining of coal resources [19-20].

Given the limited research on the recharge sources and evolutionary processes of groundwater in this region, this paper aims to bridge the gap by conducting systematic sampling and testing analysis in the Anle Mining Area, combining multivariate statistical analysis, Piper trilinear diagrams, Gibbs diagrams, and isotopic techniques to thoroughly investigate the recharge sources, recharge periods, and hydrogeochemical evolution processes of groundwater. This research holds significant guidance for the development, utilization, and protection of karst water resources in the mining area.

## 2. Study Area

### *2.1. General Setting*

The research region is situated in Anle Village, Jinjiang Town, Shangri-La City, positioned within a deeply cut high and steep mountain landscape. The main peak of the mountains in the northeast is over 4000 m above the sea level, while the valley floor in the south is at an elevation of 1860 m,

resulting in a relative elevation difference of more than 2300 meters. The study area features significant topographic relief and distinct vertical climatic zoning, characterized by a three-dimensional climate with frequent changes between sunny and cloudy weather, as well as large temperature variations. The lowest temperature recorded is -5°C, and the highest is 30°C, primarily occurring from June to September. The average annual rainfall is 985 mm, with the frost and ice period spanning from December to March of the year. The research area is part of the Jinsha River basin, with the principal river being the Anle River, which flows from the northwest to the southeast into the Jinsha River. The dry season flow rate is 6.58 $m^3/s$, and the wet season flow rate reaches 8.79 $m^3/s$. The Anle River serves as the local base level for erosion, while other gullies and streams show significant differences in flow rates between the rainy and dry seasons.

### *2.2. Geological and Hydrogeological Setting*

The study area is positioned on southwestern limb of a northwest trending anticline, namely the AnlePingzi anticline. The core of the anticline is made up by the Middle to Upper Cambrian series, the flanks are formed by Devonian and Carboniferous strata. The western limb is intact, but the eastern limb is disrupted by faults, forming a nearly symmetrical, overturned short-axis anticline. The Anlepingzi anticline is further bounded by 4 faults (Figure 1), including a NW-SE trending fault dipping towards the SW (F1), a NE-SW trending fault dipping towards the NW (F2), a NW-SE trending fault dipping towards the SE (F3), and a near E-W trending fault dipping towards the south (F4). The eastern part of the study area features a groundwater watershed, with four faults acting as impermeable boundaries to the north. The western and southern sides serve as discharge areas, constituting a complete hydrogeological unit.

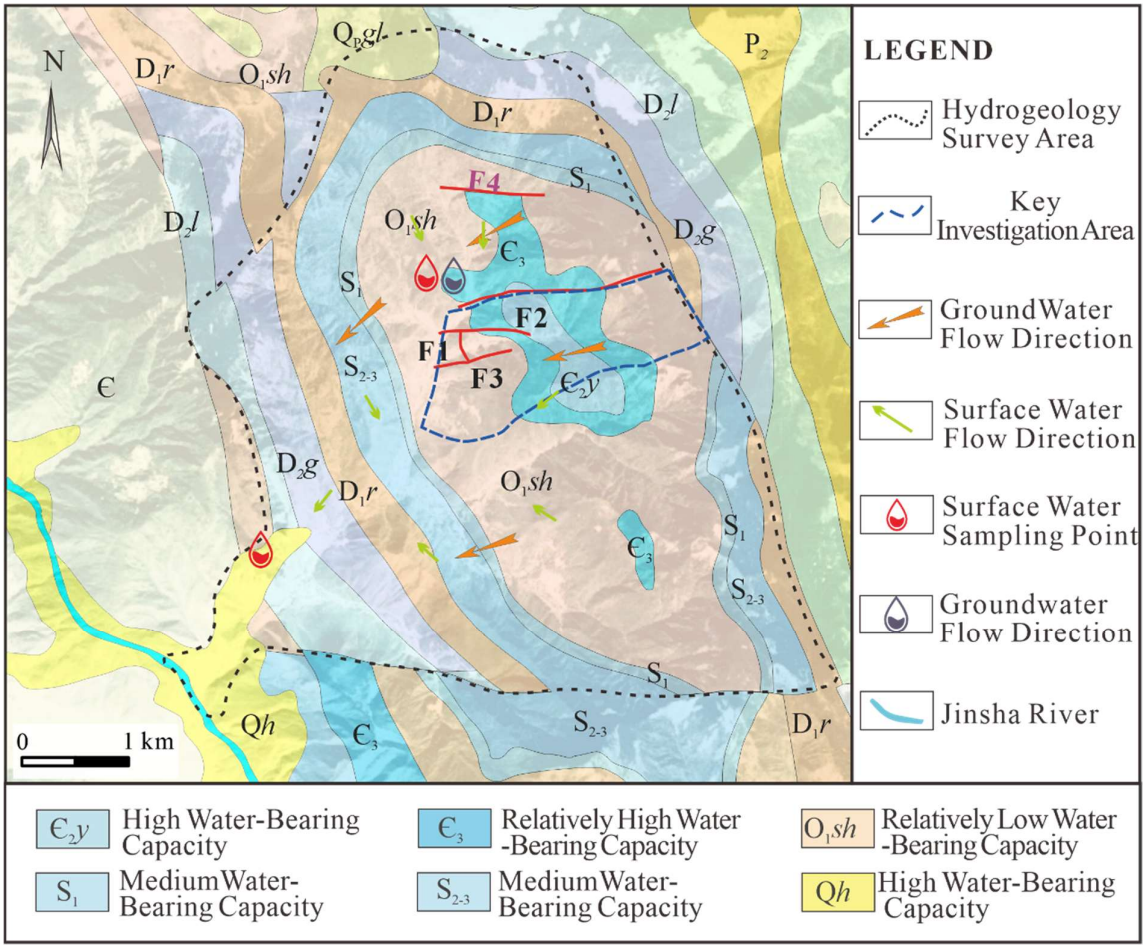


**Fig. 1.** The hydrogeological sketch map of the Anle mining area.

The study area exposes more than 6,800 meters of carbonate rock formations intercalated with clastic rocks and nearly 200 meters of molasse formations, including strata from the Cambrian, the Ordovician, the Silurian, the Devonian, the Carboniferous, and the Quaternary. The groundwater in the region is classified into porous water in loose rocks, karst water in carbonate rocks, and fissure water in bedrock. From bottom to top, the primary aquifers in the study area are the Middle Cambrian Yinchuangou Formation karst-fissure aquifer, the Upper Cambrian karst-fissure aquifer, the Quaternary alluvial-diluvial porous aquifer, and the Quaternary residual slope deposit porous aquifer. The region is dominated by widely exposed carbonate rock karst water. The rock layers generally exhibit poorly developed karren and clint, with relatively well-developed fractures. The surface often shows weathered, knife-cut-like karst features, which are conducive to groundwater recharge, flow, and discharge.

The study area barely detected surface water, with atmospheric precipitation being the primary source of groundwater recharge. Temporary surface runoff from atmospheric precipitation percolates along river valleys, creating linear recharge zones. The recharge zones are found in the exposed dolomite fractures and structural zones of the mine. Fractured aquifers and hydraulic structures are interspersed within the unit. Owing to the intensely dissected topography and structural conditions, groundwater mainly moves through interlayer fractured zones, fractures, and hydraulic structures within the aquifer. It typically discharges through advantageous structural positions via faults (such as f2), with a minor portion discharging as springs.

In the mining area, the aquifer possesses well-developed fractures, and the rock exhibits high permeability, facilitating unobstructed groundwater flow. Moreover, the mining operations have resulted in a vast mined-out area that extends to significant depths, interconnected by inclined shafts. The groundwater from the surrounding rock aquifer of the ore body converges in large volumes into the existing lowest mining pit through tunnels and inclined shafts, creating an artificial discharge area. It is then discharged into the Anle River through the mine.

## 3. Materials and Methods

### *3.1. Sampling*

On purpose of thoroughly study the sources of groundwater recharge and the evolution process of groundwater in the Anle mining area, based on a detailed investigation on the hydrogeological conditions of the study area, systematic sampling was carried out on rainy season in April 2024. A total of 10 samples were collected along the groundwater flow direction from the northeast to the southwest of the AnlePingzi anticline (Figure 1). Four karst groundwater samples in the mining zone were collected, including two contaminated samples (ID: 24KD001; ID: 24KD002) and two diverted clean groundwater samples (ID: 24KD003; ID: 24KD004), two surface water samples from this mining zone (ID: 24DB001, 24DB002) were also collected, the rest four sampling points were arranged along the upper reaches of the Jinsha River up to the Xiaolongtan drinking water protection zone (ID: 24DB003 to 24DB006), ensuring that the sampled locations could reflect the changes in the regional water environment.

To ensure the accuracy of the major and trace elements and stable isotopic analysis, the sampling methodology was conducted strictly in accordance with the 'Water quality Technical regulation on the design of sampling programmes (HJ 495-2009)' and 'Water Quality-Guidance on sampling techniques (HJ 494-2009)', polyethylene plastic and glass bottles were adapted for elements and isotopic testing, respectively. Before sampling, the sampling bottles were rinsed 2~3 times with raw water samples, then quickly filled with 555 mL of pre-rinsed polyethylene plastic bottles, tightened the caps, and labeled., all samples were filtered through 0.45 μm membrane filters, then were stored at 4 °C until analysis for testing.

### *3.2. Analytical Methods*

Anions and Cations testing were conducted at the Kunming Prospecting Design Institute. $K^+$, $Na^+$, $Ca^{2+}$, $Mg^{2+}$ were analyzed using Inductively Coupled Plasma Optical Emission Spectrometer iCAP PRO (precision, ±1%), $Cl^-$, $SO_4^{2-}$, $NO^{3-}$ were tested using Ion Chromatography ECO-863 (precision, ±1%). The analysis of hydrogen ($\delta^2H$) and oxygen ($\delta^{18}O$) compositions was conducted using a liquid water isotope analyzer (GSPC-I126) at Beijing Qingxi technology research institute, the international reference standard Vienna Standard Mean Ocean Water (V-SMOW, ‰) were employing for testing. The testing precisions were ±1.0 ‰ for $\delta^2H$ and ±0. 2‰ for $\delta^{18}O$.

## 4. Results and Discussion

The hydrochemical data were processed using SPSS Statistics 22 in conjunction with Excel 2016, and Piper trilinear plots, Gibbs diagrams, and ionic ratio charts were drew using Origin 2022.

### *4.1. Hydrochemical Characteristics and Their Sources of Recharge*

4.1.1. Statistical Characteristics of Ionic Hydrochemistry. The statistical results of hydrochemical indicators for karst groundwater and surface water in the study area are shown in Table 1. As is illustrated, all pH values from the ground water and uncontaminated samples were slightly higher than 7.0, suggesting their alkaline nature. The TDS of ground water samples ranged from 54.00~223.00 mg/L, with an average of 164.38 mg/L, while the uncontaminated samples ranged from 182.00~162.00 mg/L, with an average of 172.00 mg/L, indicating that compositional sources of surface water and groundwater are basically consistent.

The order of abundance of cation concentrations (expressed in mg/L) were $Ca^{2+} > Mg^{2+} > Na^+ > K^+$, while those of the anions (expressed in mg/L) were $HCO_3^- > SO_4^{2-} > NO^{3-} > Cl^-$. A synthesis study monitoring the variations of ground water on $K^+$, $Na^+$, $Mg^{2+}$, $Cl^-$, $SO_4^{2-}$, and $NO^{3-}$ has revealed that those irons change significantly due to the acceleration urbanization and industrialization, the variable coefficient is being used as an indication of influences of human activities on hydrochemical components. As is shown in Table 1, the surface water and uncontaminated groundwater exhibits relatively low variable coefficient of $K^+$, $Na^+$, $Mg^{2+}$, and $NO^{3-}$, suggesting that the samples in the study area have rarely been affected by mining or agriculture. The $Ca^{2+}$ and $HCO_3^-$ show relatively small variations, indicating that both surface water and uncontaminated groundwater are influenced by the weathering and dissolution processes of carbonate rock aquifers and other rocks.

As for the contaminated groundwater samples, pH values show significantly decrease with mean values at 1.88, suggesting the water exhibits a very strong acidity. The TDS ranged from 44800~49300 mg/L, with mean value of 47050 mg/L, indicating high concentration of dissolved solids. The order of abundance of cation concentrations (expressed in mg/L) were $Mg^{2+} > Ca^{2+} > K^+ > Na^+$, while those of the anions (expressed in mg/L) were $SO_4^{2-} >> NO^{3-} > Cl^-$. The results show high correlations with feature of contaminated water.

**Table 1.** Statistics of hydrochemical characteristics of surface water and groundwater in the study area

| Type | Item | pH | TDS | K+ | Na+ | Ca2+ | Mg2+ | Cl- | SO42- | HCO3- | NO3- |
|---|---|---|---|---|---|---|---|---|---|---|---|
| Contaminated Groundwater (n=2) | Minimum value | 1.68 | 44800.00 | 41.70 | 29.10 | 413.00 | 735.00 | 0.49 | 18578.00 | Nd | 4.77 |
| | Maximum value | 2.08 | 49300.00 | 42.00 | 33.20 | 432.00 | 798.00 | 0.58 | 24030.00 | Nd | 13.50 |
| | Mean value | 1. | 47050. | 41.8 | 31.1 | 422. | 766. | 0.5 | 21304.0 | Nd | 9.14 |

| | | | | | | | | | | | |
|---|---|---|---|---|---|---|---|---|---|---|---|
| | | 88 | 00 | 5 | 5 | 50 | 50 | 4 | 0 | | |
| | Standard deviation | 0.28 | 3181.98 | 0.21 | 2.90 | 13.44 | 44.55 | 0.07 | 3855.15 | Nd | 6.17 |
| | Coefficient of variation | 0.15 | 0.07 | 0.01 | 0.09 | 0.03 | 0.06 | 0.12 | 0.18 | Nd | 0.68 |
| Uncontaminated Groundwater (n=2) | Minimum value | 7.77 | 162.00 | 0.42 | 26.30 | 0.36 | 19.80 | 0.11 | 47.20 | 118.00 | 0.08 |
| | Maximum value | 7.90 | 182.00 | 0.64 | 26.30 | 0.41 | 23.60 | 0.12 | 51.30 | 126.00 | 0.08 |
| | Mean value | 7.84 | 172.00 | 0.53 | 26.30 | 0.39 | 21.70 | 0.11 | 49.25 | 122.00 | 0.08 |
| | Standard deviation | 0.09 | 14.14 | 0.16 | 0.00 | 0.04 | 2.69 | 0.01 | 2.90 | 5.66 | 0.00 |
| | Coefficient of variation | 0.01 | 0.08 | 0.29 | 0.00 | 0.09 | 0.12 | 0.06 | 0.06 | 0.05 | 0.00 |
| Surface Water (n=6) | Minimum value | 7.32 | 54.00 | 0.36 | 11.00 | 0.30 | 5.36 | 0.24 | 3.28 | 53.00 | 0.40 |
| | Maximum value | 7.65 | 223.00 | 0.75 | 29.20 | 2.68 | 14.50 | 0.45 | 17.20 | 160.00 | 0.73 |
| | Mean value | 7.54 | 161.83 | 0.47 | 21.97 | 1.24 | 10.10 | 0.37 | 8.52 | 107.17 | 0.60 |
| | Standard deviation | 0.13 | 62.58 | 0.14 | 6.95 | 0.93 | 3.66 | 0.10 | 5.01 | 39.44 | 0.11 |
| | Coefficient of variation | 0.02 | 0.39 | 0.30 | 0.32 | 0.75 | 0.36 | 0.27 | 0.59 | 0.37 | 0.19 |

Note: pH and the Variable coefficient are dimensionless; the units for the rest are mg/L

4.1.2. Hydrochemical Type. Water chemistry type in this study was determined according to the Shukalev classification, among the 10 water samples, three hydrochemical types were identified. Two uncontaminated underground water samples are of the $HCO_3^-$-$SO_4^{2-}$-$Ca^{2+}$-$Mg^2$ type, the contaminated underground samples are of $SO_4^{2-}$-$Mg^2$ type. Six surface water samples are $HCO_3^-$-$Ca^{2+}$-$Mg^2$ type. Overall, the surface water in the study area is primarily of the $HCO_3^-$-$Ca^{2+}$ type. The groundwater has a certain influence on downstream surface water. The upstream groundwater is mainly $SO_4^{2-}$ type, controlled by topographical factors, transitioning to the downstream where it is influenced by the dissolution of carbonate minerals. In the study area, the chemical composition of surface water is jointly controlled by leached $HCO_3^-$ and $Ca^{2+}$ ions and $SO_4^{2-}$ and $Mg^{2+}$ ions.

Piper trilinear diagram, unaffected by human factors, relies on the natural chemical composition of the water, making it objective and is widely used to classify the hydrochemical types. As shown in Figure 2, in terms of anions, the distribution pattern of uncontaminated groundwater and surface water samples are concentrated in the middle and lower corner of the right triangle, indicating that $HCO_3^-$ is the dominant anion. while most contaminated samples showed the dominance of the $SO_4^{2-}$ type. Moreover, most of the surface samples in the lower left side of the diamond-shaped field located in the middle of $Ca^{2+}$ and $Mg^2$, the surface sample of the mining area show more concentration of $Mg^2$. The groundwater sample is clearly showed the dominance of the $SO_4^{2-}$ type.

The hydrochemical type was relatively simple. The ion concentrations and hydrochemical types increased from the recharge area to the discharge area, indicating that rock–water interaction was strengthened. However, influenced by mining activities and human activities, the hydrochemical types of surface water and groundwater exhibited diverse characteristics

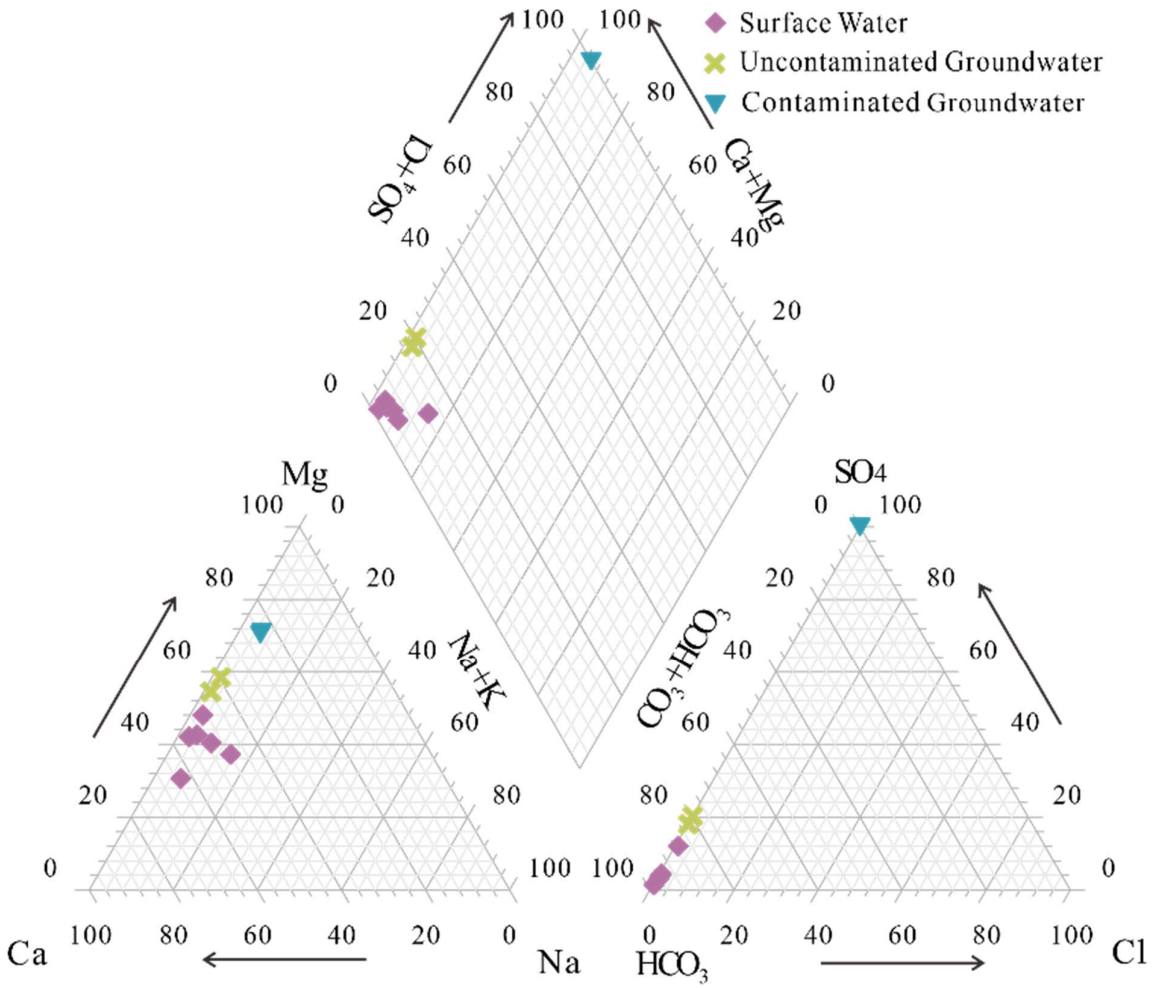


**Fig. 2.** The Piper diagram of ground water and surface water samples.

### *4.2. Hydrochemical Characteristics and Their Sources of Recharge*

Hydrogen and oxygen stable isotopes are commonly used to identify the sources of groundwater recharge, determine the transformation processes, and are important parameters for the formation and evolution of water cycles.

The analysis of $\delta D$ and $\delta^{18}O$ values for water samples in the study area shows that the $\delta D$ and $\delta^{18}O$ of the contaminated groundwater are between -96.9 ‰~-94.93 ‰, and -12.61‰ -12.39‰, respectively, with average values of -95.92 ‰~-12.5 ‰; the $\delta D$ and $\delta^{18}O$ of the uncontaminated groundwater are between -104.84 ‰ and -103.94 ‰, and -14.31 ‰ -14.27 ‰, respectively, with average values of -104.39 ‰ and -14.39 ‰; the $\delta D$ and $\delta^{18}O$ of surface water are between -102.2 ‰~-92.59 ‰, and -14.08 ‰ -13.08 ‰, respectively, with average values of -96.2 ‰ -13.49 ‰. The ranges of d-excess (d) values for the three sampling types are at 3.98 ‰~4.19 ‰, 9.64 ‰~10.22 ‰, and 10.44 ‰~12.28 ‰, with average values at 4.09 ‰, 9.93 ‰, and 11.69 ‰, respectively (Table 2).

**Table 2.** Analytical results of hydrogen and oxygen isotope of water samples in the study area

| Sample Number | δDV-SMOW/‰ | δ18OV-SMOW/‰ | d/‰ | ρ(Cl-)/mg·L-1 |
|---|---|---|---|---|
| 24KD-01 | -96.9 | -12.61 | 3.98 | 0.584 |
| 24KD-02 | -94.93 | -12.39 | 4.19 | 0.491 |
| 24KD-03 | -104.84 | -14.31 | 9.64 | 0.118 |
| 24KD-04 | 103.94 | -14.27 | 10.22 | 0.109 |
| 24DB-05 | -93.93 | -13.2 | 11.67 | 0.235 |
| 24DB-06 | -92.59 | -13.08 | 12.05 | 0.4 |
| 24DB-07 | -96.28 | -13.57 | 12.28 | 0.451 |
| 24DB-08 | -96.29 | -13.52 | 11.87 | 0.438 |
| 24DB-09 | -95.88 | -13.46 | 11.8 | 0.448 |
| 24DB-10 | -102.2 | -14.08 | 10.44 | 0.258 |

The $\delta D$ and $\delta^{18}O$ values of uncontaminated groundwater and surface water in the study area are above the Global Meteoric Water Line (GMWL) (Figure 3), indicating that the primary source is atmospheric precipitation, but evaporation may have affected the water during precipitation and infiltration processes, leading to isotopic enrichment. The $\delta^{18}O$ values of surface water is higher compared to the uncontaminated groundwater. In study area, the carbonate minerals such as dolomite and calcite are well developed, and these minerals have higher $\delta^{18}O$ values, which in turn affect the $\delta^{18}O$ values of the water bodies. Additionally, the formation and decomposition of carbonate minerals can influence the isotopic composition of water bodies, especially in areas with intense evaporation, these processes may lead to an increase in the $\delta^{18}O$ values of water bodies. Isotope data in this study can infer that there may be a certain hydraulic connection between uncontaminated groundwater and surface water.

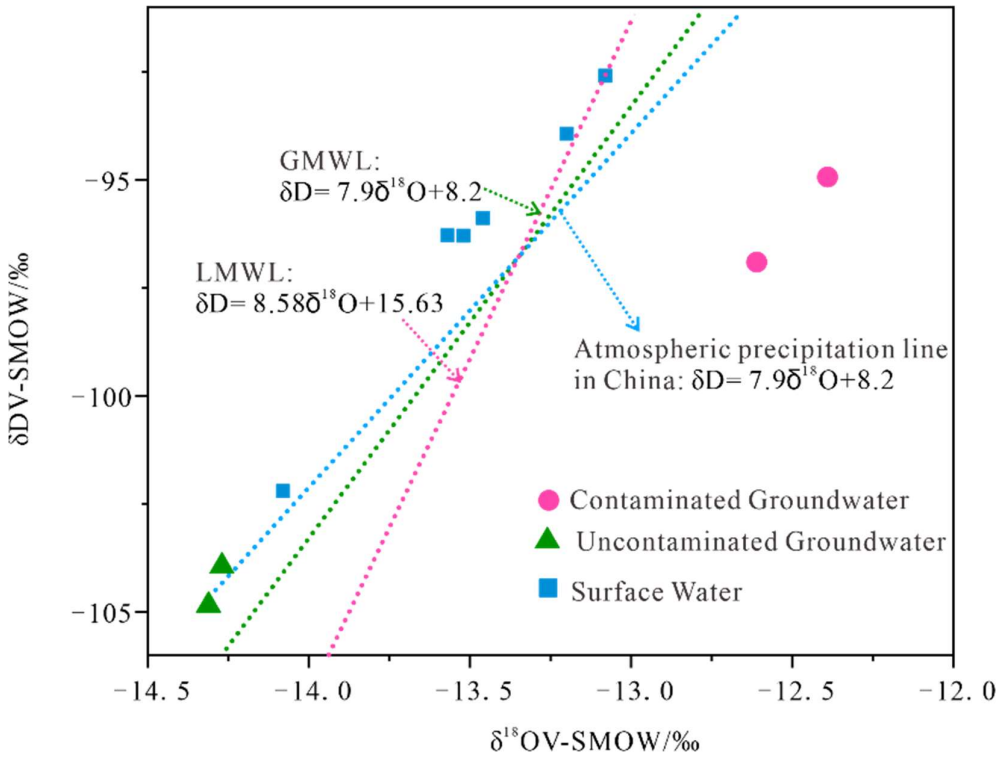


**Fig. 3.** Relationship between contaminated groundwater, uncontaminated groundwater and surface water δD-δ18O in the study area

The deuterium excess (d-excess) parameter is a measure of the degree of evaporation and condensation balance of atmospheric precipitation in environment. Generally, the d-excess value is mainly controlled by the humidity of the air, intensive evaporation could show negative d-excess values. Comparing the average d-excess values of uncontaminated groundwater and surface water, both values significantly deviate from the global average value of atmospheric precipitation (10 ‰) (Table 2).

The relationship between $Cl^-$ and $\delta^{18}O$ has a certain indicative role in the migration process of groundwater. The relationship between Cl- and $\delta^{18}O$ in the water environment shows the following trends:

1) A sharp increase in $Cl^-$ concentration with little change in $\delta^{18}O$, which is the result of the combination of dissolution and evaporation;

2) Little change in $Cl^-$ concentration with a sharp increase in $\delta^{18}O$, reflecting the impact of evaporation on the water environment; because evaporation causes a significant change in δ18O while moderately altering $Cl^-$ concentration;

3) A clear correlation between $Cl^-$ and $\delta^{18}O$, with $\delta^{18}O$ enriching in the direction of increasing $Cl^-$ concentration, reflecting the control of evaporation concentration effects on the water body.

Relationship between $\delta^{18}O$ and $Cl^-$ of studying sample is shown in Figure 4. Based on the enrichment of $\delta^{18}O$, the relationship between $Cl^-$ and $\delta^{18}O$ in uncontaminated groundwater and surface water can be divided into two groups. Group A is enriched in $\delta^{18}O$, with $Cl^-$ mass concentrations being close to each other. The second group shows an overall increase in $Cl^-$ mass concentration with the increase of $\delta^{18}O$ values. As is illustrated in Figure 4, the concentration of $Cl^-$ in the surface water of the study area is significantly higher than that in the uncontaminated groundwater, suggesting that human activities are likely the main cause of the higher Cl- concentrations.

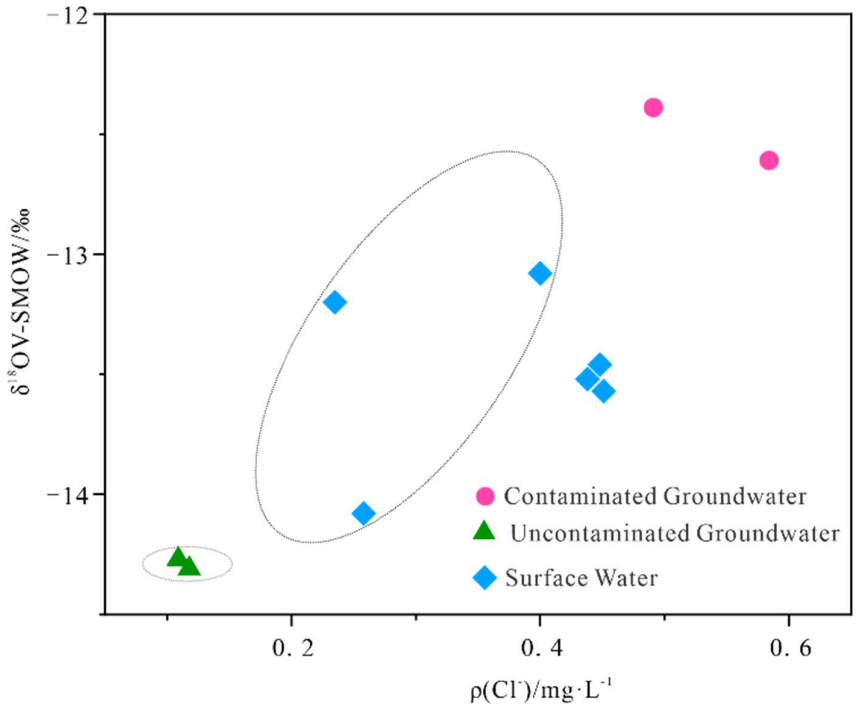


**Fig. 4.** Relationship between δ18O and ρ(Cl-) in contaminated, ncontaminated groundwater and surface water

### *4.3. Mechanisms of Hydrochemical Component Evolution*

4.3.1. Water-Rock Interaction. The ion ratios concentrations can straightforwardly reflect the formation mechanisms and sources of major ions in groundwater. These ratios can reveal the influence

of different sources, such as rock weathering, mineral dissolution, and other geological processes, as well as identify the potential impacts of human activities on water quality. The Gibbs diagram, plots TDS against the weight ratios of $Na^+/(Na^+ + Ca^{2+})$ or $Cl^-/(Cl^- + HCO_3^-)$, offers insights into the factors affecting natural water chemistry and to reflect the primary mechanisms of hydrochemical formation. Hydrochemical data of groundwater and surface water from this study area were plotted on a Gibbs diagram, the results are shown in Figure 5.

The values of $Na^+/(Na^+ + Ca^{2+})$ and $Cl^-/(Cl^- + HCO_3^-)$ for both groundwater (including uncontaminated and contaminated water samples) and surface water in the study area are less than 0.2, nevertheless the uncontaminated groundwater in $Cl^-/(Cl^- + HCO_3^-)$ show values close to 1, because of the HCO3- in uncontaminated groundwater falls below the detection limit. Approximately, all surface and uncontaminated groundwater samples points are primarily located near the TDS axis in the middle of the Gibbs diagram, concentrated in the rock weathering control region (Figure 5), indicating that the major ionic composition of surface and uncontaminated water in the study area is predominantly controlled by rock weathering processes, the evaporative concentration might have a minor contribution to the sources of ions of the uncontaminated groundwater.

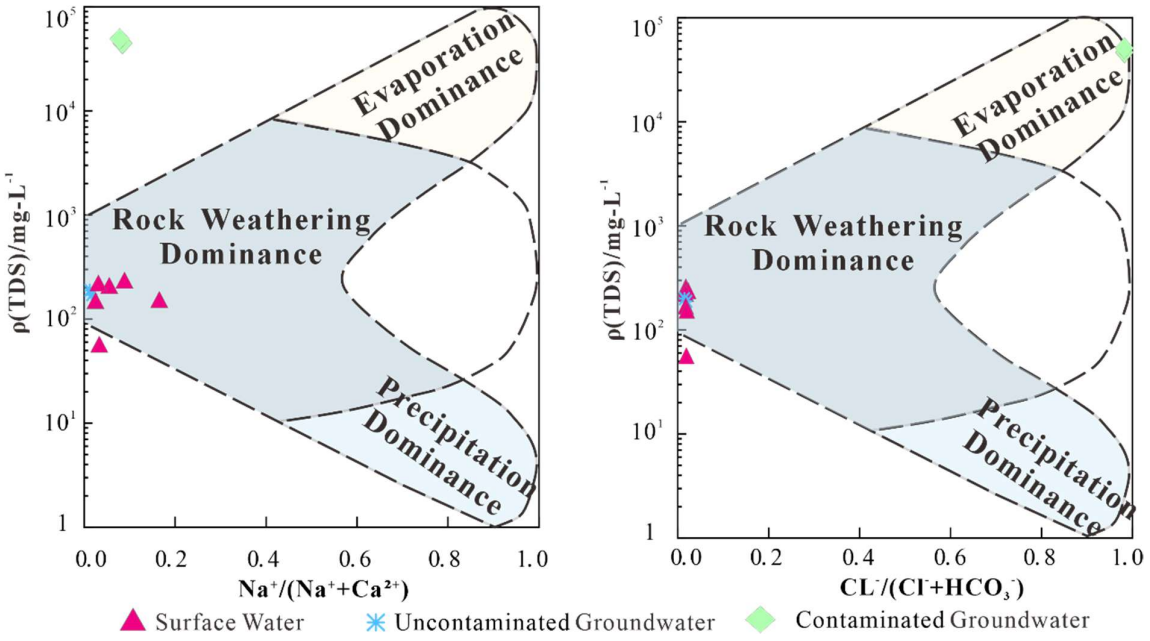


**Fig. 5.** The Gibbs diagram for karst groundwater and surface water in the study area.

4.3.2. Ion Exchange Process. Under specific conditions, particles can adsorb certain cations and simultaneously release previously adsorbed cations into the water. This cation exchange process can alter the hydrochemical composition of natural waters. The milliequivalent concentration ratio of $[Na^+ - Cl^-]/[(Ca^{2+} + Mg^{2+}) - (SO_4^{2-} + HCO_3^-)]$ is commonly indicate exchange within the water body, if cation exchange occurs, the ratio of these two values is generally around -1. Most of the surface water and uncontaminated groundwater samples showed positive correlation, with a correlation coefficient of 0.75 and a slope of -0.84, close to -1 (Figure 6(a)), indicating cation exchange processes in the of water the study area. But the groundwater shows negative correlation, suggesting relatively different cation exchange processes comparing with the surface water and uncontaminated groundwater.

The Schoeller indices (CAI-I and CAI-II) can illustrate ion exchange between groundwater and its associated aquifer. The indices help to assessing the chemical progression of groundwater. If the $Ca^{2+}$ or $Mg^{2+}$ ions in groundwater have exchanged with $Na^+$ ions in the aquifer minerals, the CAI-I and CAI-II values are less than 0. Conversely, if $Na^+$ ions in groundwater are exchanged with $Ca^{2+}$ or $Mg^{2+}$ in the aquifer minerals, the indices would show values greater than 0. A higher absolute value

of these indices signifies a more substantial degree of ion exchange. The ion exchange reactions can be expressed by the following equations (Equations (1) and (2)):

$$CAI\text{-}I = Cl^- - (Na^+ + K^+)/Cl^- \quad (1)$$

$$CAI\text{-}II = Cl^- - (Na^+ + K^+)/(HCO_3^- + SO_4^{2-} + CO_3^{2-} + NO^{3-}) \quad (2)$$

Based on the analysis of the Schoeller indices (CA-I and CA-II) of the studying samples (Figure 6(b)), it can be observed that the cation exchange process in the water samples of the study area is not pronounced, with significant deviations in contaminated groundwater values. All surface water and uncontaminated groundwater samples exhibit value greater than 0, which may be closely related to sulfate and ferric sulfate solutions from contaminated groundwater. The dissolution of carbonates by sulfuric acid leads to an increase in the concentrations of $Ca^{2+}$ and $Mg^{2+}$ in water, approaching saturation. Therefore, the surface water and uncontaminated groundwater in the study area, affected by upstream high $SO_4^{2-}$, exhibits negative cation exchange characteristics.

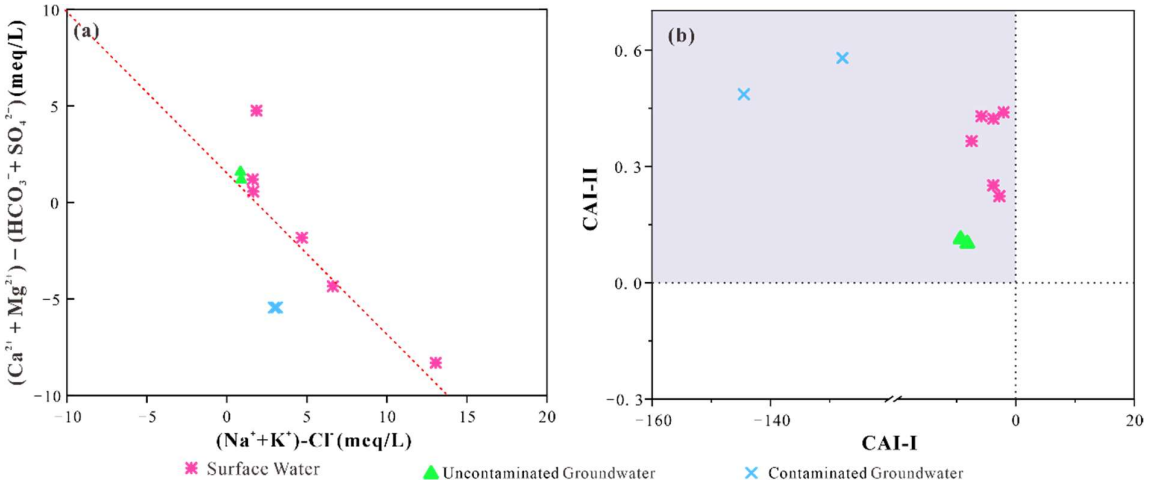


**Fig. 6.** Ploting of (a) [Na+-Cl-]/[(Ca2++Mg2+) -(SO42-+HCO3-)], (b) CAI-I vs. CAI-II

4.3.3. Mineral Dissolution Process. Groundwater undergoes long-term hydrogeochemical reactions with the aquifer rocks, and during this process, the ratio of various ions can reveal the sources and evolution of the main ions in the water environment.

The proportional coefficient map of ion composition in the study area is shown in Figure 7(a), most of the water sample points are distributed near the 1:1 line. If the ratio of $N(Ca^{2+}+Mg^{2+})/N(HCO_3^-+SO_4^{2-})$ is close to 1, then $Ca^{2+}$ and $Mg^{2+}$ are likely derived from the dissolution of carbonate and sulfate minerals such as calcite, dolomite, and gypsum; if the ratio is greater than 1, there should also be silicate dissolution. Therefore, the main factors influencing the hydrochemical characteristics of the uncontaminated groundwater and surface water in the study area are the weathering and dissolution of carbonates and sulfates, and the hydrochemical characteristics are also affected by silicate dissolution.

As shown in Figure 7(b), the sample points of uncontaminated groundwater and surface water are generally located above the 2:1 and 1:1 line. When the $N(Ca^{2+})/N(Mg^{2+})$ value is close to 1, it indicates that the dissolved carbonate minerals are mainly dolomite, and the dissolution of calcite will increase the ratio; if the ratio is greater than 2, there is also the dissolution of silicates. Therefore, the dissolved carbonate minerals in the uncontaminated groundwater and surface water of the study area are calcite and dolomite, with only one surface water sample showing silicate weathering characteristics. As shown in Figure 7(c), most of the water sample points are below the 1:1 line. When the $Na^+$-$Cl^-$ relationship deviates from the 1:1 line, it indicates that Na+ is derived from other processes.

The weathering of silicates and the dissolution of potassium feldspar and sodium feldspar are the main sources of $HCO_3^-$. As is shown in Figure 7(d), the water sample points are generally below and near the 1:1 line, and combining this with the previous discussion, the $HCO_3^-$ in the surface water and uncontaminated groundwater of the study area mainly derives from the weathering of silicates.

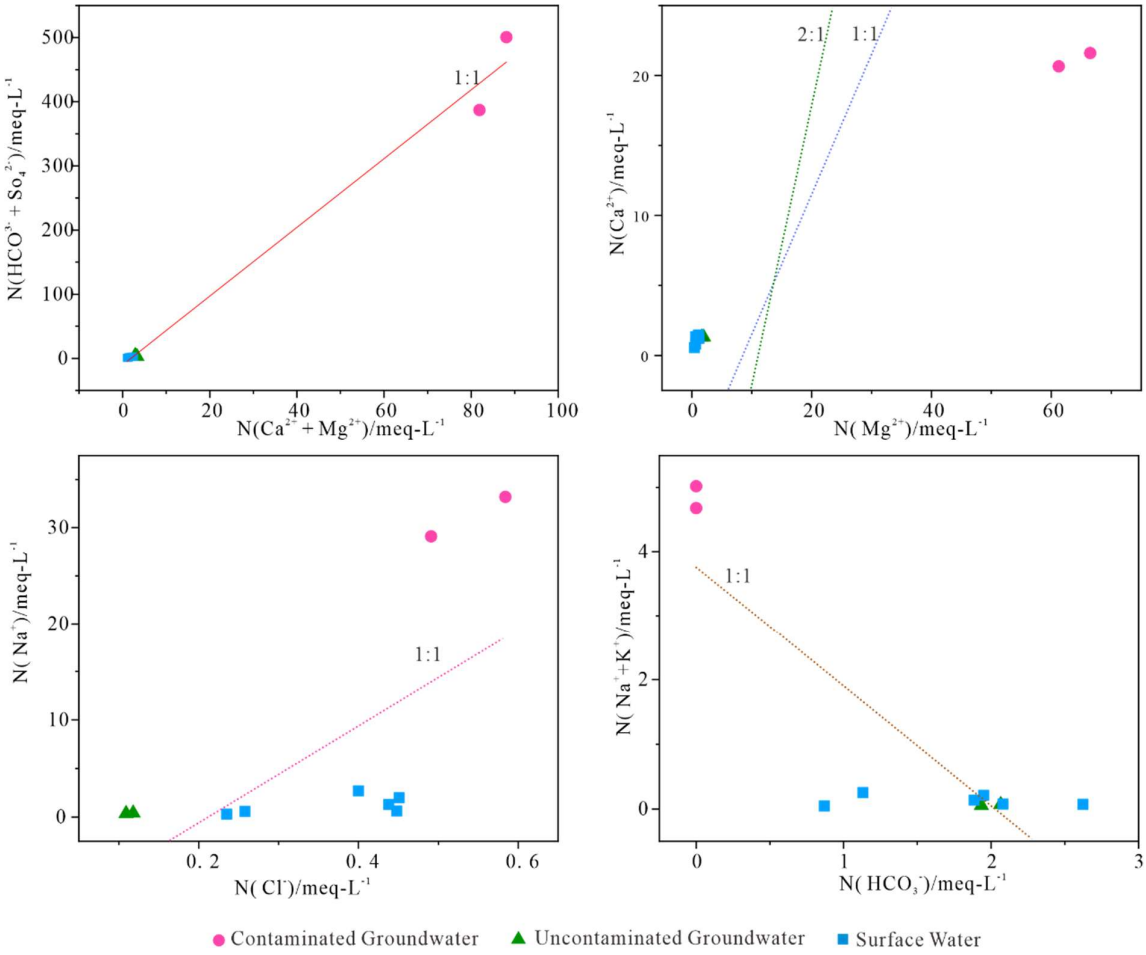


**Fig. 7.** Relationship between different ions in contaminated, uncontaminated groundwater and surface water

4.3.4. Human Activities. Nitrate is one of the most common pollutants in water. The concentration of $\rho(NO^{3-})$ is generally below 10 mg·L-1 in natural water bodies, but it is characterized by high solubility and ease of migration. With the impact of human activities, the mass concentration of $NO^{3-}$ in water bodies can increase, thus nitrate in water can generally indicate the impact of human activities on hydrochemistry. Improper use of fertilizers and pesticides in agriculture, random discharge of domestic sewage and industrial wastewater, etc., are all important causes of nitrate pollution in groundwater. As is illustrated in Table 1, the distribution and variation of nitrate content follow the pattern: polluted groundwater > surface water > unpolluted groundwater. Therefore, the nitrate in the surface water of the study area may originate from the agricultural nitrogen fertilizers used in the process of cultivated land planting, while the contaminated groundwater is related to the development of mineral resources.

## 5. Conclusions

1) The contaminated groundwater, uncontaminated groundwater and surface water show different hydrochemical characteristics, the pH value for each sample show means values at 1.88, 7.84 and 7.54. The contaminated groundwater is acidic, while the uncontaminated groundwater and surface water

are generally slightly alkaline. The TDS of contaminated groundwater exhibits hard water quality with a high number of impurities, while TDS of the rest samples show mean values between 172 and 161.83. The cation and anion of contaminated groundwater is dominated by $Ca^{2+}$, $Mg^{2+}$ and $SO_4^{2-}$, respectively. In the remaining samples, the cations are mainly $Na^{+}$ and $Mg^{2+}$, with the anions dominated $HCO_3^{-}$ and $SO_4^{2-}$. The uncontaminated underground water samples are of the $HCO_3^{-}$-$SO_4^{2-}$-$Ca^{2+}$-$Mg^{2}$ type, the contaminated underground samples are of $SO_4^{2-}$-$Mg^{2}$ type. the water samples are $HCO_3^{-}$-$Ca^{2+}$-$Mg^{2}$ type.

2) The characteristics of hydrogen and oxygen isotopes and the deuterium excess indicate that the unpolluted karst groundwater and surface water in the study area are primarily replenished by atmospheric precipitation and are also influenced by evaporation. The surface water is most significantly affected by the intensity of evaporation, leading to a higher enrichment of heavy isotopes in the surface water samples.

3) The hydrochemical evolution of uncontaminated karst groundwater and surface water in the study area is mainly influenced by the weathering and dissolution of carbonate rocks, sulfate rocks, and silicate rocks. The surface water and uncontaminated groundwater of the study area mainly derives from the weathering of silicates. The concentration of $\rho(NO^{3-})$ of the surface water of the study area may related to agricultural fertilizers, and contaminated groundwater is highly related to the development of mineral resources.

## References


[1] Lipczynska-Kochany, E. (2018). Effect of climate change on humic substances and associated impacts on the quality of surface water and groundwater: A review. Science of the total environment, 640, 1548-1565.

[2] Burri, N. M., Weatherl, R., Moeck, C., & Schirmer, M. (2019). A review of threats to groundwater quality in the anthropocene. Science of the Total Environment, 684, 136-154.

[3] Schwartz, F. W., & Zhang, H. (2024). Fundamentals of groundwater. John Wiley & Sons.

[4] Marandi, A., & Shand, P. (2018). Groundwater chemistry and the Gibbs Diagram. Applied Geochemistry, 97, 209-212.

[5] Jasechko, S. (2019). Global isotope hydrogeology—Review. Reviews of Geophysics, 57(3), 835-965.

[6] Sasakova, N., Gregova, G., Takacova, D., Mojzisova, J., Papajova, I., Venglovsky, J., ... & Kovacova, S. (2018). Pollution of surface and ground water by sources related to agricultural activities. Frontiers in Sustainable Food Systems, 2, 42.

[7] Wang, H., Zhan, J., Yao, W., Wang, B., Deng, S., Huang, J., ... & Wang, Y. (2018). Comparison of pharmaceutical abatement in various water matrices by conventional ozonation, peroxone (O3/H2O2), and an electro-peroxone process. Water research, 130, 127-138.

[8] Selvam, S., Jesuraja, K., Venkatramanan, S., Roy, P. D., & Kumari, V. J. (2021). Hazardous microplastic characteristics and its role as a vector of heavy metal in groundwater and surface water of coastal south India. Journal of Hazardous Materials, 402, 123786.

[9] Michael, H. A., Post, V. E., Wilson, A. M., & Werner, A. D. (2017). Science, society, and the coastal groundwater squeeze. Water Resources Research, 53(4), 2610-2617.

[10] Li, P., Tian, R., & Liu, R. (2019). Solute geochemistry and multivariate analysis of water quality in the Guohua phosphorite mine, Guizhou Province, China. Exposure and Health, 11, 81-94.

[11] Krause, S., Lewandowski, J., Grimm, N. B., Hannah, D. M., Pinay, G., McDonald, K., ... & Turk, V. (2024). Ecohydrological interfaces as hotspots of ecosystem processes. Ecohydrological Interfaces, 1-28.

[12] Driscoll, C. T., & Postek, K. M. (2020). The chemistry of aluminum in surface waters. In The environmental

chemistry of aluminum (pp. 363-418). CRC press.

[13] Deutsch, W. J., & Siegel, R. (2020). Groundwater geochemistry: fundamentals and applications to contamination. CRC press.

[14] Kasonga, T. K., Coetzee, M. A., Kamika, I., Ngole-Jeme, V. M., & Momba, M. N. B. (2021). Endocrine-disruptive chemicals as contaminants of emerging concern in wastewater and surface water: A review. Journal of Environmental Management, 277, 111485.

[15] Akhtar, N., Syakir Ishak, M. I., Bhawani, S. A., & Umar, K. (2021). Various natural and anthropogenic factors responsible for water quality degradation: A review. Water, 13(19), 2660.

[16] Riser-Roberts, E. (2020). Remediation of petroleum contaminated soils: biological, physical, and chemical processes. CRC press.

[17] Xu, B., Liu, S., Zhou, J. L., Zheng, C., Weifeng, J., Chen, B., ... & Qiu, W. (2021). PFAS and their substitutes in groundwater: Occurrence, transformation and remediation. Journal of hazardous materials, 412, 125159.

[18] Quesada, H. B., Baptista, A. T. A., Cusioli, L. F., Seibert, D., de Oliveira Bezerra, C., & Bergamasco, R. (2019). Surface water pollution by pharmaceuticals and an alternative of removal by low-cost adsorbents: A review. Chemosphere, 222, 766-780.

[19] Edokpayi, J. N., Odiyo, J. O., & Durowoju, O. S. (2017). Impact of wastewater on surface water quality in developing countries: a case study of South Africa. Water quality, 10(66561), 10-5772.

[20] Li, P., Karunanidhi, D., Subramani, T., & Srinivasamoorthy, K. (2021). Sources and consequences of groundwater contamination. Archives of environmental contamination and toxicology, 80, 1-10.